

This work was written as part of one of the author's official duties as an Employee of the United States Government and is therefore a work of the United States Government. In accordance with 17 U.S.C. 105, no copyright protection is available for such works under U.S. Law. Access to this work was provided by the University of Maryland, Baltimore County (UMBC) ScholarWorks@UMBC digital repository on the Maryland Shared Open Access (MD-SOAR) platform.

Please provide feedback

Please support the ScholarWorks@UMBC repository by emailing scholarworks-group@umbc.edu and telling us what having access to this work means to you and why it's important to you. Thank you.

Plasmonic Brewster Angle: Broadband Extraordinary Transmission through Optical Gratings

Andrea Alù,^{1,*} Giuseppe D'Aguanno,^{2,3} Nadia Mattiucci,^{2,3} and Mark J. Bloemer³

¹*Department of ECE, University of Texas at Austin, Austin, Texas 78712, USA*

²*Nanogenesis Division, AEGIS Technologies, Huntsville, Alabama 35806, USA*

³*Department of the Army, Charles M. Bowden Facility, Redstone Arsenal, Alabama 35898, USA*
(Received 16 November 2010; revised manuscript received 13 January 2011; published 23 March 2011)

Extraordinary optical transmission through metallic gratings is a well established effect based on the collective resonance of corrugated screens. Being based on plasmonic resonances, its bandwidth is inherently narrow, in particular, for thick screens and narrow apertures. We introduce here a different mechanism to achieve total transmission through an otherwise opaque screen, based on an ultrabroadband tunneling that can span from dc to the visible range at a given incidence angle. This phenomenon effectively represents the equivalent of Brewster transmission for plasmonic and opaque screens.

DOI: 10.1103/PhysRevLett.106.123902

PACS numbers: 42.79.Dj, 41.20.Jb, 42.25.Ja, 71.45.Gm

The phenomenon of extraordinary optical transmission (EOT) through thin slits or apertures in a thick metal screen has been widely analyzed in the past decade [1]. The ratio of optical energy tunneling through an otherwise opaque screen versus the energy effectively impinging on the apertures may be made dramatically larger than unity, in particular, for smaller apertures and larger periods. This anomalous transmission is based on multiple factors, including the excitation of plasmonic and Fabry-Perot (FP) resonances and other resonant effects supported by the periodicity of the corrugations [1]. A new class of optical devices based on EOT has been envisioned, such as light-emitting diodes, selective polarization filters, and energy concentrators. One of the drawbacks of EOT for several of these applications is associated with the inherently narrow bandwidth of operation, which is directly associated with the resonant mechanisms on which it is based, in particular, with the excitation of plasmonic and FP resonances. This becomes particularly relevant for smaller apertures and thicker screens, which are usually associated with larger Q -factor resonances. On the contrary, as long as the array period is rather small (below the first Bragg resonance), the EOT response is rather independent on the incidence angle. Here we introduce a dual EOT mechanism, inherently non-resonant, which may provide analogous levels of transmission enhancement over ultrabroad bandwidths, but for specific incidence angles. We show that this phenomenon is the analog of Brewster transmission for corrugated plasmonic screens, providing minimized reflection for transverse-magnetic (TM) polarization, weakly dependent on frequency and on the screen thickness but selective to the incidence angle. Independent of our findings, a recent Letter has reported broadband transmission through narrow slits in the IR regime, based on spoof-surface plasmons [2]. Our results extend these findings, showing that ultrabroadband transmission may be achieved without necessarily relying on plasmon resonances but rather exploiting a nonresonant Brewster-like effect based on impedance matching.

Consider the geometry of Fig. 1: A metallic screen of thickness l , corrugated by slits of width w and period d , is illuminated by a TM wave. The scattering from such a periodic structure is modeled here by using a transmission-line (TL) approach, analogous to Ref. [3]. Because of the array periodicity, we can model the diffraction problem as its circuit analog depicted in the bottom of Fig. 1, in which the free-space regions are modeled as semi-infinite TL and the slit region is treated as a TL segment of length l . For a given angle of incidence θ with respect to the z axis, the effective vacuum wave number is $\beta_0 = k_0 \cos\theta$, i.e., the longitudinal component of the impinging wave vector, the characteristic impedance per unit length is $Z_0 = \eta_0 d \cos\theta$, calculated as the ratio between the voltage across one period $V_0 = \int_0^d E_x dx = |\mathbf{E}| d \cos\theta$ and the current per unit length $I_0 = H_y = |\mathbf{H}|/\eta_0$, and $\eta_0 = \sqrt{\mu_0/\epsilon_0}$ is the vacuum impedance. Inside each slit, modal propagation does not depend on the incidence angle. The wave number β_s and characteristic impedance per unit length Z_s satisfy the equations [4]

$$\tanh[\sqrt{\beta_s^2 - k_0^2 w/2} \sqrt{\beta_s^2 - k_0^2}] = -\sqrt{\beta_s^2 - k_0^2} \epsilon_m / \epsilon_m, \quad (1)$$

$$Z_s = w\beta_s / (\omega\epsilon_0),$$

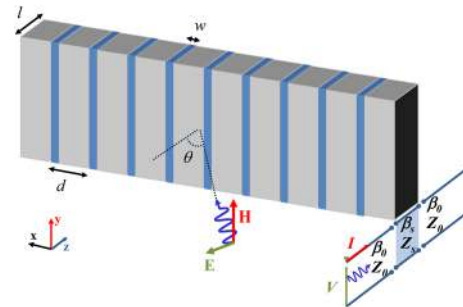


FIG. 1 (color online). The geometry of interest and its equivalent TL model.

where ε_m is the relative permittivity of the metal and Z_s is the ratio between $V_s = \int_0^w E_x dx = E_x w$ and $I_s = H_y = \omega \varepsilon_0 E_x / \beta_s$. In deriving Eq. (1), we have assumed that the field penetration in the metal is very small, but we fully take into account the finite conductivity of the plasmonic material, its frequency dispersion, and possible absorption. This TL model holds as long as only the dominant TM mode propagates inside the slit and only the zero diffraction order radiates in free space, i.e., $w \ll d < \lambda_0 = 2\pi/k_0$. In such circumstances, with good approximation the boundary conditions at the grating entrance and exit require that the equivalent voltages and currents are continuous, as in the circuit model in Fig. 1. More refined TL models [3] may consider also the presence of parasitic reactive elements at the two interfaces, taking into account the energy stored in the evanescent diffraction orders and in the guided modes excited at the grating discontinuity, as well as the possible excitation of TE modes and the coupling among the slits. As we show in the following, these second-order effects are not significant in modeling the mechanisms described here.

In the limit of ultranarrow slits $w \ll d$, the effective slit impedance Z_s is inherently small compared to Z_0 for normal incidence, which physically corresponds to expectedly large reflections from such a grating. The reflection coefficient at the grating entrance is generally written as

$$R = \frac{[Z_s^2 - Z_0^2] \tan(\beta_s l)}{[Z_s^2 + Z_0^2] \tan(\beta_s l) + 2iZ_s Z_0}. \quad (2)$$

In the lossless limit, zero reflection and EOT are obtained at the usual FP resonances $\beta_s l = n\pi$, with n being an integer, consistent with the findings in Ref. [1]. EOT resonances are also achieved when the grating period allows coupling to surface plasmons or spoof-surface plasmons for corrugated conducting screens [5]. This phenomenon is not captured by Eq. (2), since it involves higher-order propagating diffraction orders, which arise only for periods comparable to or larger than λ_0 . Yet, Eq. (2) admits another peculiar condition for zero reflection, which arises when $Z_s = Z_0$, i.e., when the grating is anomalously *impedance matched* with free space. For normal incidence this condition is hardly met, due to the opaqueness of metal, but, by increasing the angle of incidence θ , Z_0 is smoothly reduced to zero as the tangential component of the electric field is reduced. From Eq. (1), the anomalous matching condition is achieved at the incidence angle θ_B :

$$\cos\theta_B = (\beta_s w)/(k_0 d), \quad (3)$$

which represents the effective *plasmonic Brewster angle*. This anomalous matching phenomenon is *totally independent* of the grating thickness, since the effective slit impedance matches the impinging wave at each interface, producing anomalous total tunneling and energy squeezing through each slit. This strikingly simple formula captures to a large degree a novel tunneling phenomenon. Different

from FP and plasmon resonances [1,2], minimum reflection is achieved even when significant absorption is present in the slits, of great interest for energy concentration and harvesting. In addition, condition (3) is weakly dependent on frequency, ensuring that this Brewster-like transmission provides an ultrabroadband response, effectively extending from zero frequencies (dc) to the breakdown of this model $d \simeq \lambda_0$. For lower frequencies, the metal tends to become a perfect conductor, for which $\beta_s = k_0$ and $\theta_B = \cos^{-1}(w/d)$, close to the grazing angle for small w/d . For higher frequencies, the plasmonic features of metal come into play, increasing β_s and correspondingly reducing θ_B .

It is important to stress that this effect is based on the modal propagation in ultranarrow slits, and it is therefore limited to 2D apertures (slits). In some sense, this phenomenon is the dual of the energy squeezing and total transmission mechanism through ultranarrow channels filled with zero-permittivity materials [6]. In Ref. [7], this effect was proven to be based on an analogous matching phenomenon, for which the inherently low impedance in an ultranarrow channel may be matched to a much thicker waveguide by using zero-permittivity fillings. Here, we can equivalently describe the wave interaction with the narrow slits as the one of an homogenized metamaterial slab with relative effective parameters $\varepsilon_{\text{eff}}^{(s)} = d/w$ and $\mu_{\text{eff}}^{(s)} = w(\beta_s^2/k_0^2 + \sin^2\theta)/d$. For small ratios w/d , $\varepsilon_{\text{eff}}^{(s)}$ is very large while $\mu_{\text{eff}}^{(s)}$ is comparably low. However, at the plasmonic Brewster angle (3), the effective impedance $\sqrt{\mu_{\text{eff}}^{(s)}/\varepsilon_{\text{eff}}^{(s)}} \cos\theta_r = Z_s/d$ (where θ_r is the refracted angle in the effective material) coincides with the one in vacuum Z_0/d , producing unitary transmission. Different from Refs. [6,7], here we do not need to fill the slits with zero-permittivity metamaterials, as the outside medium naturally holds a very low impedance for large angles. This tunneling mechanism is the *exact physical analog* of what happens in a dielectric slab with $\varepsilon > \varepsilon_0$ at the Brewster angle condition, for which the lower impedance of a dielectric etalon may be matched to free space for TM incidence at an oblique angle. Brewster-like effects for metallic gratings have been discussed in the literature [8] but referring to quite different transmission mechanisms, mainly based on collective plasmonic resonances, largely frequency-dependent. Here, due to the absence of a resonance, this matching mechanism is inherently ultrabroadband, as we verify in the following with full-wave simulations.

In Fig. 2, we show the calculated angular TM power transmission spectra for a grating with $l = 200$ nm, $d = 96$ nm, and various slits widths, as indicated in each panel. The left column shows full-wave simulations based on the Fourier modal method [9], compared in the right to our analytical model. We consider realistic experimental dispersion and loss of silver permittivity [10]. It is noticed how the TL model captures with extreme accuracy the

fundamental physical mechanisms behind the transmission resonances of the grating. At normal incidence ($\theta = 0$), typical EOT peaks based on FP resonances are visible in all panels. For narrower slits (top row), such resonances are shifted to lower frequencies, due to their plasmonic features that ensure a larger $\text{Re}[\beta_s]$ for smaller w in (1). These resonances reflect in horizontal bands in the plots in Fig. 2, since this EOT mechanism is inherently narrowband in frequency but weakly dependent on the incidence angle.

In contrast, the plasmonic Brewster transmission arises in all plots as a vertical band, confirming weak dependence on frequency but strong selectivity to the transmission angle. Each plot reports, as a dashed line, the dispersion of the predicted Brewster angle (or, better, its real part, since losses are considered here), as in Eq. (3). For smaller ratios w/d the plasmonic Brewster angle is closer to grazing, whereas for larger widths it moves towards smaller angles. The weak dispersion of the dashed line is due to the variation of $\text{Re}[\beta_s]$ with frequency, which somehow limits the bandwidth of this effect, and is followed with excellent precision by the transmission peak in the calculated full-wave spectra. For higher frequencies, the effect of absorption in the slit is evident, in particular, for narrower widths, which reduces the transmission maxima. In any case, an ultrabroadband EOT phenomenon is verified by our full-wave simulations precisely at the angle θ_B . We have verified that, by further increasing the slit aperture for a fixed period, the vertical transmission band shifts to smaller θ_B ,

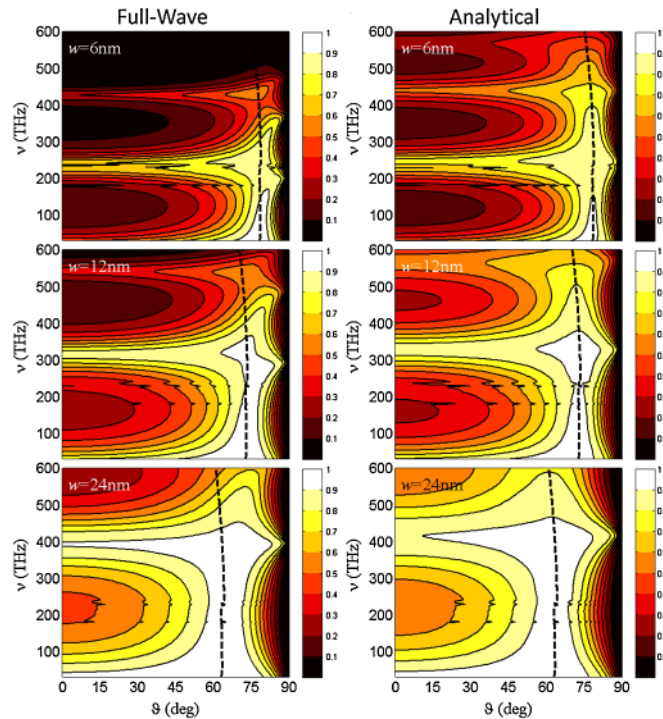


FIG. 2 (color online). Angular transmission spectra for a grating thickness $l = 200$ nm and period $d = 96$ nm. The slit width is indicated in each panel. Fourier modal method simulations (left) are compared with analytical results (right). The dashed line indicates the plasmonic Brewster angle condition.

judiciously following Eq. (3), even for very large slit apertures. Such extreme scenarios are of less interest, since the angular selectivity of the grating is compromised and energy squeezing is limited. In the supplemental material [11], we show a similar plot but considering a larger grating period $d = 192$ nm. The results are consistent with Fig. 2, and also here Brewster transmission is obtained over a broad frequency range from dc to the visible at the specific angle θ_B . In this second scenario, since the silver filling ratio is larger, angular selectivity and loss sensitivity are increased, due to larger energy squeezing.

Figure 3 shows analogous results but for a thicker screen $l = 400$ nm. As expected, the horizontal transmission bands typical of FP resonances have narrower bandwidths and are denser along the frequency spectrum, due to longer slits. However, the anomalous Brewster transmission is weakly affected by the thickness, as confirmed by Eq. (3), since minimal reflection is expected at the entrance and exit faces of the screen, independent of the frequency of operation. Transmission is slightly reduced at higher frequencies in this example, due to the longer propagation through narrow slits.

Anomalous transmission would be available even if, at some section along the slit, we would add a matched absorbing material or an energy harvesting device, converting the tunneled energy into other forms. On the contrary, FP or plasmon resonances, based on multiple reflections or coupling between the slit entrance and exit [1,2], would be completely dampened under such a condition. This provides interesting venues to apply this matching phenomenon for energy concentration and harvesting.

In order to further highlight the anomalous features of this phenomenon, Fig. 4(a) shows the electric field amplitude (transverse to the slit) for the geometry of Fig. 3 (bottom row) at the frequency $f = 395$ THz, which represents the frequency of the second FP resonance of the

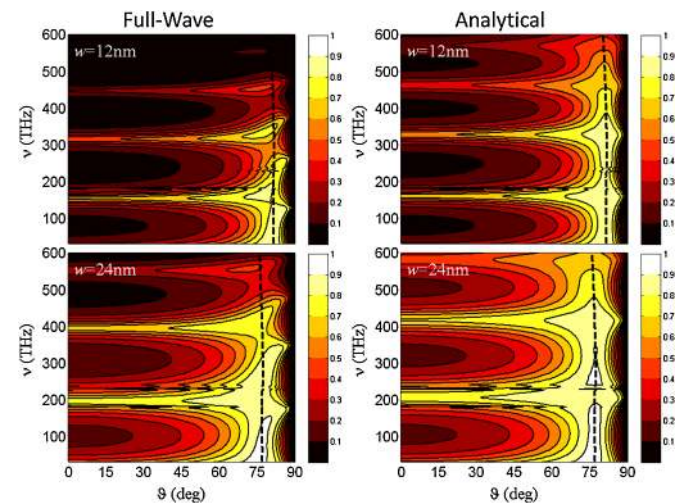


FIG. 3 (color online). Similar to Fig. 2 but for thicker screens and a larger period: $l = 400$ nm and $d = 192$ nm.

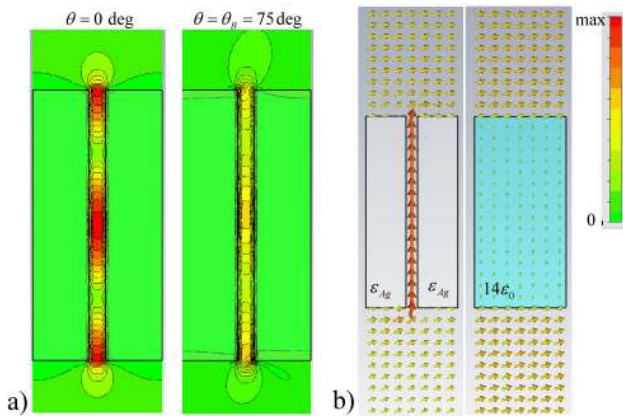


FIG. 4 (color online). (a) Electric field distribution E_x on the E plane for $l = 400$ nm, $d = 192$ nm, and $w = 24$ nm at $f = 395$ THz for normal incidence (left) and incidence angle $\theta_B = 75^\circ$ (right). (b) Power flow distribution at the Brewster angle (left) and comparison with an equivalent dielectric etalon with $\epsilon = 14\epsilon_0$. In each panel, the fields are normalized to the same scale.

grating ($\text{Re}[\beta_s]l = 2\pi$). In the left panel, we show the case of normal incidence excitation, whereas in the right panel we excite at the Brewster angle $\theta_B = 75^\circ$. It is evident how, even if both excitations ensure very high transmission, the field distributions inside the slit are very different. For normal incidence, total transmission is obtained by exploiting a strong FP resonance established via the large mismatch at the entrance and exit face, which forms a typical standing wave distribution inside the slit. Obviously, this resonance is very sensitive to the geometry of the slit, the operating frequency, and the presence of absorption along the slit. In contrast, at the Brewster condition, tunneling is based on impedance matching: The wave does not experience any change in effective impedance, and it can tunnel through the slit with nearly uniform amplitude and minimum reflections. For the sake of comparison, the scale in the two plots is the same, showing that the lack of resonance also reduces the peak field values in the slit and the associated stored energy, with obvious advantages in terms of robustness to loss and geometry variations. Consistent with Fig. 3, at this angle EOT is weakly dependent on frequency and the possible presence of absorption or change in the slit length. Even possible bending within the slit would not affect this matching behavior, allowing energy rerouting [6].

In Fig. 4(b), we compare the power flow (Poynting vector) distribution at the Brewster condition with the one of an equivalent dielectric etalon with the same length and $\epsilon = 14\epsilon_0$, which would support Brewster transmission at the same angle θ_B . Indeed, the slit openings in the plasmonic screen provide a tunneling mechanism that has analogous features to the usual Brewster phenomenon, despite the opaqueness of the material forming the screen. Similar to a dielectric etalon, total transmission is obtained

only for TM polarization. In fact, due to the choice of narrow slits, transverse-electric excitation would be totally reflected at all angles and all frequencies, ensuring strong polarization sensitivity, which may be used to realize ultrathin and ultrabroadband filter polarizers. In conclusion, we have shown here that plasmonic gratings formed by ultranarrow slits and small periods may support ultrabroadband anomalous matching, analogous to Brewster transmission, despite the metal opaqueness. These results may be applied to novel polarization filters, energy concentrators, and absorbers. Ultranarrow slits in plasmonic screens with aspect ratios similar to those considered in this Letter may be obtained with advanced nanofabrication techniques, such as nanoskyving [12]. Moreover, by relaxing the requirements on the slit width and period, analogously broadband transmission mechanisms may be verified from dc to terahertz frequencies. In preparation for an experimental proof of concept of this anomalous phenomenon, we have also considered the presence of a glass substrate at the grating exit, verifying that its presence does not significantly influence the previous results.

This work has been supported by ARO with STTR W31P4Q-09-C-0652, by NSF with CAREER Grant No. ECCS-0953311 to A. A., by an AFOSR YIP grant to A. A., and by ONR MURI No. N00014-10-1-0942 to A. A.

*alu@mail.utexas.edu

- [1] T. W. Ebbesen *et al.*, *Nature (London)* **391**, 667 (1998); F. J. García de Abajo, *Rev. Mod. Phys.* **79**, 1267 (2007); F. J. Garcia-Vidal *et al.*, *Rev. Mod. Phys.* **82**, 729 (2010).
- [2] X. R. Huang, R. W. Peng, and R. H. Fan, *Phys. Rev. Lett.* **105**, 243901 (2010).
- [3] F. Medina, F. Mesa, and R. Marques, *IEEE Trans. Microwave Theory Tech.* **56**, 3108 (2008).
- [4] A. Alù and N. Engheta, *J. Opt. Soc. Am. B* **23**, 571 (2006).
- [5] J. B. Pendry, L. Martin-Moreno, and F. J. Garcia-Vidal, *Science* **305**, 847 (2004).
- [6] M. Silveirinha and N. Engheta, *Phys. Rev. Lett.* **97**, 157403 (2006); B. Edwards *et al.*, *Phys. Rev. Lett.* **100**, 033903 (2008).
- [7] A. Alù, M. G. Silveirinha, and N. Engheta, *Phys. Rev. E* **78**, 016604 (2008); A. Alù and N. Engheta, *Phys. Rev. Lett.* **103**, 043902 (2009).
- [8] L. B. Mashev, E. Popov, and E. G. Loewen, *Appl. Opt.* **28**, 2538 (1989); E. Popov, S. Enoch, and N. Bonod, *Opt. Express* **17**, 6770 (2009).
- [9] L. Li, *J. Opt. Soc. Am. A* **13**, 1870 (1996), and references therein.
- [10] E. D. Palik, *Handbook of Optical Constants of Solids* (Academic, New York, 1991).
- [11] See supplemental material at <http://link.aps.org/supplemental/10.1103/PhysRevLett.106.123902> for a figure similar to Fig. 2, but for double period $d = 192$ nm.
- [12] Q. Xu, R. M. Rioux, M. D. Dickey, and G. M. Whitesides, *Acc. Chem. Res.* **41**, 1566 (2008).